Stable carbon isotope ratio of secondary particulate organic matter formed by photooxidation of toluene in indoor smog chamber

Satoshi Irei [a,b,*], Jochen Rudolph [a], Lin Huang [b], Janeen Auld [a], Donald Hastie [a]

[a] Centre for Atmospheric Chemistry and Department of Chemistry, York University, 4700 Keele St., Toronto, Ontario M3J 1P3, Canada
[b] Climate Chemistry Measurements and Research Section, Climate Research Division, Atmospheric Science and Technology Directorate, Science and Technology Branch, Environment Canada, 4905 Dufferin St., Toronto, Ontario M3H 5T4, Canada

ARTICLE INFO

ABSTRACT

Laboratory studies were conducted for stable carbon isotope ratio for secondary particulate organic matter (POM) formed by photooxidation of toluene. Using an 8 m^3 indoor YorkU smog chamber, three POM generation experiments were carried out under room temperature, atmospheric pressure, and RH < 6%. In this study, the different initial conditions were set from those in the previous flow reactor study for secondary POM formed by photooxidation of toluene: introduction of seed particles, and 40–80 times lower initial toluene mixing ratios (~1900 μg m^{-3}) and ~60 times higher toluene to NO$_x$ ratios (~7), respectively. The formation of secondary POM was confirmed by the size distribution measurements of particles and the POM was collected on quartz fiber filters for carbon mass and stable carbon isotope ratio analysis. The size distribution measurements showed that the POM mass yields were between 37% and 55% at the end of experiments, while the filter analysis showed that the yields of POM carbon collected then were between 7% and 21%, implying the substantial contribution of heteroatoms. The plot of the POM carbon yields from this study and the previous study indicated that the POM carbon yields were merged into a single profile. The results of isotope measurements demonstrated that the carbon isotope fractionation at the initial reaction step was predominant in the overall carbon isotope fractionations that occur in the sequence of the reactions leading to the formation of secondary POM carbon. Using the results, novel approach for estimation of secondary POM carbon yield with stable carbon isotope ratios is proposed.

© 2010 Elsevier Ltd. All rights reserved.

1. Introduction

Airborne particulate matter (PM) has been widely studied to date due to its possible link to radiative forcing (IPCC, 2001;

Ramanathan et al., 2001; Anderson et al., 2003) as well to its adverse health effects (Dockery et al., 1993; Thurston et al., 1994). It has been known that the fraction of organic component in airborne PM, which is known as organic aerosol or particulate organic matter (POM), is substantial (Lee et al., 2003; Na et al., 2004). However, our understanding of airborne POM is still limited due to its complex composition, variety of emission sources, and variety of formation and loss processes. Particularly, understanding secondary POM, which is the POM formed from volatile organic carbons (VOCs) by atmospheric oxidation, is very limited. Therefore, elucidation of its production mechanism, identification of its major precursor VOCs and their source(s) are urgent.

Isotope measurements are a powerful tool to gain insight into reaction mechanisms and complex mixtures where concentration measurements only cannot give sufficient information for the understanding. Stable carbon isotope measurements have been applied to VOCs in atmospheric samples, and it is evident that the measurements are useful for estimation of extent of chemical reaction of VOCs (Rudolph et al., 2000; Thompson et al., 2003; Saito et al., 2002; Nara et al., 2007) as well as for identifying location of

sources of targeted VOCs (Iannone, 2008) in the atmosphere. Isotope measurements are also used for photochemical product studies and fingerprinting POM (Sakugawa and Kaplan, 1995; Fang et al., 2002; Fisseha et al., 2009a; Aggarwal and Kawamura, 2009). However, for quantitative evaluation of atmospheric isotope measurements, understanding of the kinetic isotope effect (KIE) that a reactant and its products undergo is needed. This basic understanding can be achieved by conducting laboratory studies (Irei et al., 2006; Fisseha et al., 2009b).

The objective of this study is to have a better understanding for the variation of stable carbon isotopic composition and yield of secondary POM carbon formed by the photooxidation of toluene (denoted as the toluene + OH reaction thereafter). This study is an extension of previous studies made using a flow reactor (Irei et al., 2006). The experiments were made under different initial conditions from the previous studies, and isotope ratios and yields of POM were investigated at high toluene turnover.

2. Experiment

Three smog chamber experiments (SC I–SC III) were carried out using an 8 m^3 YorkU indoor smog chamber made of a Teflon bag (Fig. 1). The chamber had a fan set inside the Teflon bag for mixing reactants effectively. Black lights were used for UV irradiation. Details of the characterization studies for the YorkU smog chamber, such as the wall-loss of POM, are discussed elsewhere (Bienenstock, 2001; Barbu, 2003). The following is a brief description of the chamber experiments.

Air from a clean air generator (Aadco 737 pure air generator, Aadco) was continuously introduced into the chamber at 2.3 L min^{-1} during the experiments. The resulting theoretical residence time was approximately 40 h, and dilution due to the 2.3 L min^{-1} air flow over an hour was less than 2%, relative to the total volume of the chamber. The pressure inside the chamber was maintained at atmospheric pressure. The following measurements were made at 5 min intervals: size distribution measurements of PM by scanning mobility particle sizer or SMPS (TSI-3071 and TSI-3760, TSI), toluene mixing ratio measurements by GC-FID

(HP 5890), as well as NO_x mixing ratios by NO_x analyzer (Model 42s, Thermo Environmental Instruments).

The initial experimental conditions, which are the conditions just before switching the UV lights on, are summarized in Table 1. Through the injection port, 20 mL of pure gaseous NO (BOC Edwards), 18 µl of liquid toluene (Sigma–Aldrich), and 250 µl of liquid isopropyl nitrite (IPN) were injected. The IPN was synthesized from isopropanol and sodium nitrite in the presence of sulfuric acid according to the procedure described by Noyes (1943). Seed particles (ammonium sulfate) were also introduced. Droplets of ammonium sulfate (0.5 g L^{-1}) were generated using a collision nebulizer, subsequently dried by passing through a silica-gel dryer tube, and then the dried ammonium sulfate seeds were introduced into the chamber for several minutes. Prior to irradiation of UV light, the chamber was left for one hour to mix the reactants. Typically, the uniform mixture was obtained within a half hour. The initial concentrations (i.e. the concentrations just before the start of UV irradiation) of NO_x, toluene, and IPN in all experiments were ~4300 µg m^{-3}, ~1900 µg m^{-3}, and ~2500 µg m^{-3}, respectively. The number concentration and the median of the size distribution for the seed particles before the UV irradiation were ~2 × 10^5 cm^{-3} and ~100 nm, respectively.

A set of two 25 mm quartz filters (Pallflex Tissuequartz, Pall Corp.) placed in series was used for filter sampling for total POM carbon and its stable carbon isotope ratio analysis. It should be noted that another set of filter sampling was simultaneously performed with 47 mm disc filters for compound-specific analysis (shown in Fig. 1), the results of which will be presented elsewhere. The filter sampling for the total POM carbon started at a flow rate of 4.7 L min^{-1} after switching the UV lights off, and the POM was collected for 5 h. During filter sampling, the out flow of the chamber was displaced with clean air in order to maintain atmospheric pressure inside the chamber.

The organic carbon collected on the filters was converted to CO_2 using a method similar to the procedure described elsewhere (Irei et al., 2006). The following modification was made: the commercially available copper oxide (99.999% purity, Aldrich) was baked at 1173 K overnight to reduce the background carbon, and then baked
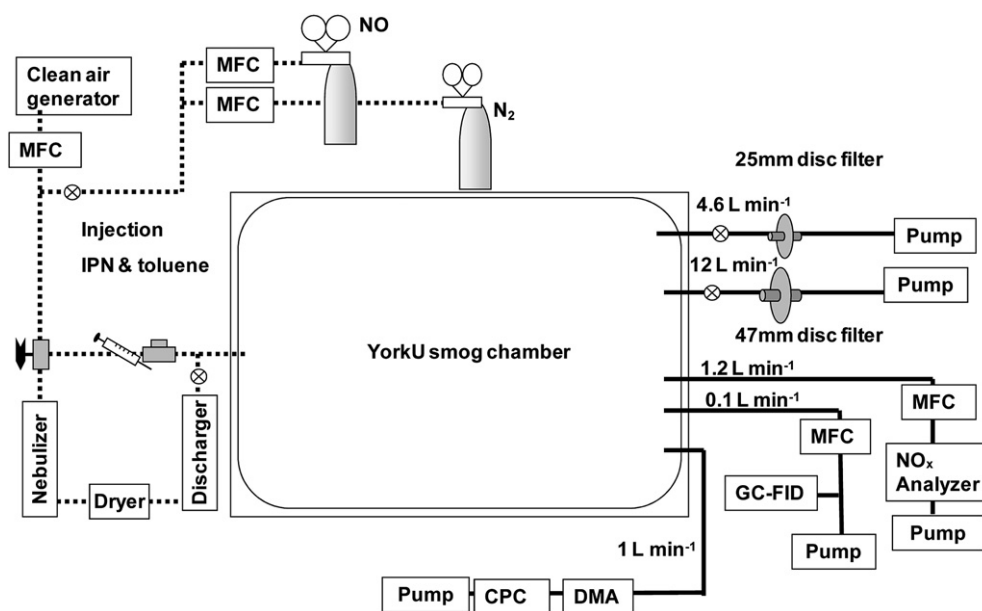

Fig. 1. Schematic of experimental setup for smog chamber experiment. The dotted and solid lines indicate inflows and outflows, respectively. See the text for toluene, NO_x, and PM measurements and filter sampling for detail.

Table 1
Initial conditions[a] of smog chamber experiments.

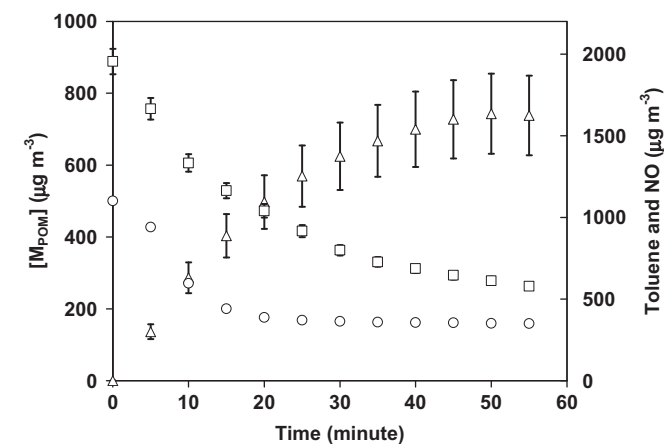| Experiment	Toluene concentration ($\mu g\,m^{-3}$)	NO_x concentration ($\mu g\,m^{-3}$)	Number concentration of seed particles (particles cm^{-3})	Median size of seed particles (nm)
SC I	1920	4400	2.1×10^5	70
SC II	1880	4300	1.8×10^5	70
SC III	1960	4300	2.5×10^5	107

[a] The conditions before the UV irradiation started.

again at 773 K for several days to re-oxidize the copper oxide. This pre-treatment substantially reduced the blank value, which was crucial for the analysis of samples with small carbon amount. The modified method was evaluated by conducting standard spike tests with 2 mg C mL^{-1} aqueous solution of the international standard, IAEA-CH-6 (sucrose). The converted CO_2 was extracted using the conventional method, and the CO_2 extracted was quantitatively measured using the method described elsewhere (Irei, 2008). The extracted CO_2 was enclosed in a Pyrex ampoule, and the stable carbon isotope ratio was measured by dual-inlet isotope ratio mass spectrometry (Isoprime, GV-instrument). All $\delta^{13}C$ measurements were made relative to the laboratory CO_2 standards prepared from carbonates, which were traceable to Vienna PeeDee Belemnite (VPDB). The traceability of the carbonates is discussed in detail elsewhere (Huang et al., 2001). Note that all the $\delta^{13}C$ values presented here are expressed as δ value in per mille (i.e. $\delta^{13}C\ (\permil) = [R_{smpl}/R_{VPDB} - 1] \times 1000$, where R_{smpl} and R_{VPDB} stand for atomic ratios of $^{13}C/^{12}C$ in the sample and that of the VPDB, respectively). Uncertainties given for the measured $\delta^{13}C$ and carbon yields here are 1σ standard errors from replicate measurements, unless otherwise noted.

3. Results and discussion

3.1. Concentration and yield

Fig. 2 shows time series plots for the wall-loss corrected mass concentration of secondary POM ([M_{POM}]), as well as for the toluene and the NO concentrations. Shown error bars are 15%, 3%, and 1% measurement uncertainties, for, toluene, and NO, respectively. Note

Fig. 2. Time series plot for POM mass ([M_{POM}], triangle), toluene (square) and NO (circle) concentrations during SC III experiment. The error bars shown are 15%, 3%, and 1% uncertainties for [M_{POM}], toluene, and NO, respectively. The UV lights were switched on and off at 0 min and 50 min, respectively.

that the [M_{POM}] was estimated according to the results of size distribution measurements and assuming a density of 1 g cm^{-3}. Our results are significantly different from the observations by others: (1) in our experiments 70% of toluene reacted within 90 min while others took several hours to have <30% of toluene reaction (Hurley et al., 2001; Sato et al., 2004), (2) in our experiments the POM mass yields (Y_M) were from 37% to 55%, while others were from ~2% to 15% (Izumi and Fukuyama, 1990; Edney et al., 2000; Hurley et al., 2001; Stroud et al., 2004). The results of the on-line measurements at the end of UV irradiation are summarized in Table 2.

Fig. 3 shows plots for [M_{POM}] and Y_M as a function of the mass concentration of toluene reacted ($\Delta[M_{C7H8}]$). In the Y_M plot, some spikes were seen in the very early stage of toluene consumption. The spikes are likely the artifact caused by small time difference between the intervals for the size distribution and the toluene concentration measurements: the rates in the production of POM and the consumption of toluene were the highest in the very early stage, and, therefore, the slightly unsynchronized measurements would result in the least reliable comparison between the D[M_{C7H8}] and the [M_{POM}] there. For this reason, the spikes in the early stage were eliminated for discussion later.

The [M_{POM}] profiles as a function of the $\Delta[M_{C7H8}]$ reproducibly showed a polynomial increase in the very early stage of oxidation, and then linear increase in the later stage. When converting to the Y_M plot, such [M_{POM}] profiles appear as linear increase in the early stage and then leveling off in the later stage. This is a typical profile observed for the secondary POM formed from the photooxidation of aromatic hydrocarbons (Izumi and Fukuyama, 1990; Odum et al., 1996; Hurley et al., 2001; Sato et al., 2004). It has been suggested that such a profile is an indication that the POM formed is made of the second generation product that is limited by the concentration of OH radical (Hurley et al., 2001). Although it has been observed in many other studies that the [M_{POM}] eventually levels off in the late stage of POM formation, which should appear as a decreasing profile in the Y_M plot, such a decreasing profile was not observed clearly here. At the end of each photooxidation experiments, the Y_M values reached the maximum of 37%, 55%, and 55% for SC I, SC II, and SC III, respectively. As referred earlier, those yields are unusually high.

3.2. Analysis of filter samples

3.2.1. Blank and measurement test with IAEA-CH-6

The isotope analysis showed that the average quantitative and $\delta^{13}C$ values for the blank filters ($n = 14$) were $(0.20 \pm 0.03)\ \mu mol\ C$ and of $(-22 \pm 1)\permil$, respectively. The standard spike tests ($n = 8$) with the solution of IAEA-CH-6 showed that the blank corrected recovery yields were between 87% and 100%, where the range of spiked carbon mass was from 14 $\mu g\ C$ to 410 $\mu g\ C$. The measured $\delta^{13}C$ values varied from $(-11.47 \pm 0.02)\permil$ to $(-10.30 \pm 0.02)\permil$, with a small systematic change: the smaller the spiked carbon, the lighter the isotope composition. The systematic bias was due to the impact of the blank carbon. Based on mass balance, a blank correction was made for each of the measured values. After the

Table 2
Summary of smog chamber experiments at end of UV irradiation.

Experiment	Irradiation time (min)	Fraction of toluene consumed (%)	POM mass concentration, [M_{POM}] ($\mu g\,m^{-3}$)	POM mass yield,[a] Y_M (%)
SC I	26	37	260	38 ± 2
SC II	82	69	747	57 ± 2
SC III	55	71	755	55 ± 2

[a] The error shown is based only on the error for toluene reacted.
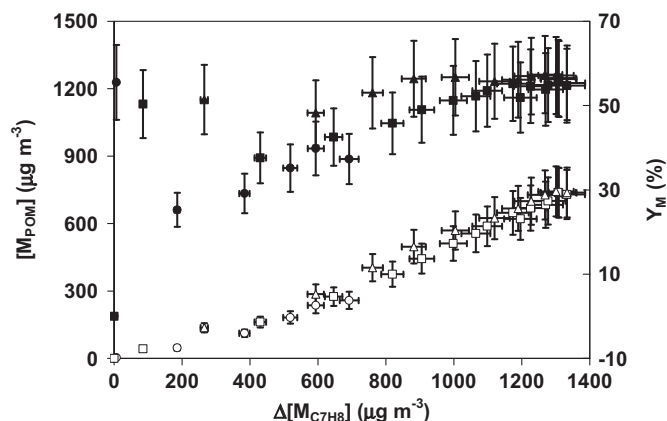
Fig. 3. Plot for POM mass concentration ([M_{POM}], open) and POM mass yield (Y_M, solid) as function of toluene mass reacted ($\Delta[M_{C7H8}]$) obtained for SC I (circle), SC II (triangle), and SC III (square) experiments. The error bars shown are 15% and 16% for the [M_{POM}] and the Y_M, respectively.

correction, the $\delta^{13}C$ values for the IAEA-CH-6 were corrected to the range from $(-10.24 \pm 0.10)‰$ to $(-9.64 \pm 0.46)‰$; more constant and accurate isotope ratios overall. However, there was still the difference of up to $(0.42 \pm 0.25)‰$ between the blank corrected isotope ratios and the reference isotope ratio, where the carbon mass was as low as 42 μg C that is almost the same carbon mass as that for the smallest sample size observed. Thus, the reader is reminded that the isotope ratios in this paper may have an offset in accuracy by $(0.42 \pm 0.25)‰$ or less.

3.2.2. Stable carbon isotope ratio

The results of filter sample analysis are summarized in Table 3. The blank corrected $\delta^{13}C$ values for the filter samples ($\delta^{13}C_{POM}$) were of significantly lighter isotopic composition than the initial isotopic composition of the precursor toluene ($^0\delta^{13}C_{C7H8}$, which was $(-27.05 \pm 0.02)‰$) by $(-2.78 \pm 0.07)‰$ up to $(-4.5 \pm 0.3)‰$, depending on the fraction of toluene consumed. These values are distinctive from the typical $\delta^{13}C$ value for fossil fuel, which is $-27‰$ approximately (Rudolph et al., 2002; Huang et al., 2006). Therefore, the results here are encouraging in that $\delta^{13}C$ measurements can be used to differentiate secondary POM from the mixture with primary POM that often comes from petroleum related emissions.

The measured $\delta^{13}C_{POM}$ values were compared with the predicted $\delta^{13}C$ values for toluene (denoted as $\delta^{13}C_{C7H8}$ thereafter) as well as for the sum of all products (denoted as $\delta^{13}C_{AllProd}$ thereafter) in Fig. 4. The predicted values were calculated using Rayleigh fractionation with $^0\delta^{13}C_{C7H8}$ of $(-27.05 \pm 0.02)‰$ and the carbon KIE of $(5.95 \pm 0.28)‰$ for the reaction of toluene with OH radical (denoted as $^{OH}\varepsilon_{C7H8}$ thereafter) reported by Anderson et al. (2004). The figure clearly demonstrates that the observed $\delta^{13}C_{POM}$ values

are almost identical to the predicted $\delta^{13}C_{AllProd}$ values. This observation was consistent with the previous findings in the flow reactor experiments (Irei et al., 2006), despite the different initial experimental conditions here: the initial toluene mixing ratios and the initial toluene/NO_x ratios for the smog chamber experiments were 40–80 times and 30–60 times lower than those in the flow reactor experiments, respectively. The consistent finding in the isotopic composition suggest several possibilities: (1) the carbon KIEs in the sequence of following reactions leading to the formation of POM is negligibly small, or (2) if there were significant KIEs in the reactions of the intermediate(s) in the gas-phase, those reactions must be completed already (i.e. the secondary POM observed is a part of the end products). According to the current understanding of carbon KIE for the reaction of OH radicals with aromatics or compounds having unsaturated bonds, it is reasonably expected that addition of OH radical to the possible intermediate(s), such as cresol, have substantial KIE (Anderson et al., 2004). Unfortunately, further speculation cannot be made with the current data set. However, these questions can be answered by conducting compound specific stable carbon isotope analysis for the secondary POM. The agreement between the $\delta^{13}C_{POM}$ and the $\delta^{13}C_{AllProd}$ also suggests two important points: (1) there is no difference in average $\delta^{13}C$ between the total POM carbon and the rest of products remaining in the gas-phase, (2) the OH-adduct channel is likely responsible for the production of the POM under our experimental conditions since the OH-adduct is responsible for the overall carbon KIE for the reaction of toluene with OH (Anderson, 2005) and the overall carbon KIE explains the observed carbon isotope ratio of total POM carbon, unless otherwise the different isotope ratios of the condensable product(s) from the OH-adduct and the H-abstract channels were cancelled out within particles and showed such an isotope ratio by coincidence.

3.2.3. POM carbon yield and carbon content

POM carbon yield (Y_C) was determined by dividing the measured POM carbon mass of filter sample (C_{POM}) by estimated carbon mass of reacted toluene in the air volume that passed through the sampling filter ($^{passed}\Delta C_{C7H8}$). The $^{passed}\Delta C_{C7H8}$ was obtained by following step-wise calculations. First, the mass of residual toluene passed through the sampling filter ($^{passed}M_{C7H8}$) was estimated based on the results of toluene concentration measurements:

$$^{passed}M_{C7H8} = \sum_{n=1}([M_{C7H8}]^n \times \Delta V^n) \tag{1}$$

where $[M_{C7H8}]^n$ is the toluene concentration determined by the nth toluene measurement since the start of filter sampling, and ΔV^n is air volume of the filter sampling during the interval between the nth and the $(n-1)$th toluene concentration measurements. $^{passed}\Delta C_{C7H8}$ was then determined as follows:

Table 3
Summary of filter sample analysis.

Experiment	$\delta^{13}C$ of POM[a]	Collected POM carbon[a]	Reacted toluene carbon passed through filter[b]	POM carbon yield[c]	POM mass loaded[d]	Carbon content[e]
	$\delta^{13}C_{POM}$ (‰)	C_{POM} (μg C)	$^{passed}\Delta C_{C7H8}$ (μg C)	Y_C (%)	$^{loaded}M_{POM}$ (μg)	(%)
SC I	-31.53 ± 0.30	47 ± 1	650 ± 80	7.3 ± 0.9	89	24 ± 3
SC II	-29.83 ± 0.07	150 ± 1	840 ± 60	18 ± 2	572	24.9 ± 0.8
SC III	-29.86 ± 0.05	198 ± 1	970 ± 70	21 ± 2	624	31.0 ± 0.6

[a] The numbers are blank corrected values for the filter samples.
[b] Estimated toluene carbon reacted that passed through sampling filter (see the text for the calculation).
[c] C_{POM} divided by $_{passed}\Delta C_{C7H8}$.
[d] POM mass loaded on the filter (see the text for the calculation).
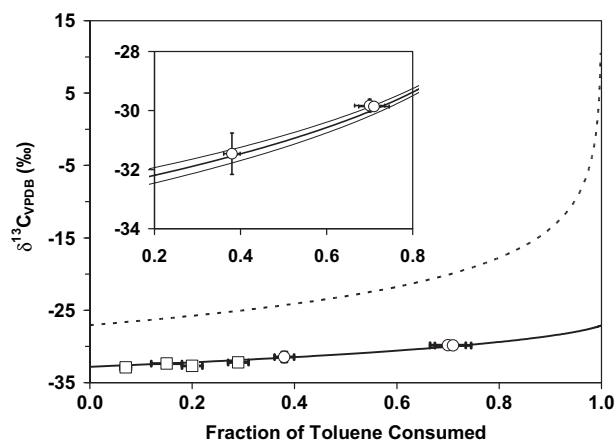[e] C_{POM} divided by $^{loaded}M_{POM}$.

Fig. 4. Plot for $\delta^{13}C$ of secondary POM as function of fraction of toluene consumed observed in smog chamber experiments (circle) and flow reactor experiments (square). The inset is the plot in an expanded scale. The data from the flow reactor experiments are adopted from Irei et al. (2006). As comparison, predicted $\delta^{13}C$ for toluene (dotted line) and the sum of all products (solid line) are also shown. See the text for calculation of the prediction in detail.

$$^{passed}\Delta C_{C7H8} = {}^{passed}M_{C7H8} \times \frac{\frac{\Delta[C_{C7H8}]}{{}^{0}[C_{C7H8}]}}{1 - \frac{\Delta[C_{C7H8}]}{{}^{0}[C_{C7H8}]}} \times \frac{7 \times 12}{92} \qquad (2)$$

where ${}^{0}[C_{C7H8}]$ is the initial toluene, concentration, $\Delta[C_{C7H8}]$ is difference in the toluene concentration between the beginning and the end of UV irradiation experiment, 7 is the carbon number of toluene, 12 is the atomic mass of carbon, and 92 is the molecular weight of toluene. Note that the term $\Delta[C_{C7H8}]/{}^{0}[C_{C7H8}]$ means the fraction of toluene consumed at the end of UV irradiation. Using the estimated $^{passed}\Delta C_{C7H8}$, the determined Y_C for the SC I, SC II, and SC III experiments were $(7.3 \pm 0.3)\%$, $(18 \pm 2)\%$, and $(21 \pm 2)\%$, respectively (Table 3). In contrast to the significantly different results for the mass yields discussed earlier, these carbon yields are of similar magnitude to literature values: $\sim 3\%$ maximum Y_C at $\sim 27\%$ fraction of toluene reacted (Izumi and Fukuyama, 1990), and Y_C in the range from 6% to 19% formed by the reaction of o-cresol (a typical first generation product from the toluene + OH reaction) with OH radical at >90% fraction of cresol reacted (Grosjean, 1984).

Fig. 5 shows plots of the Y_C as a function of fraction of toluene consumed. The figure also includes the published Y_C results using

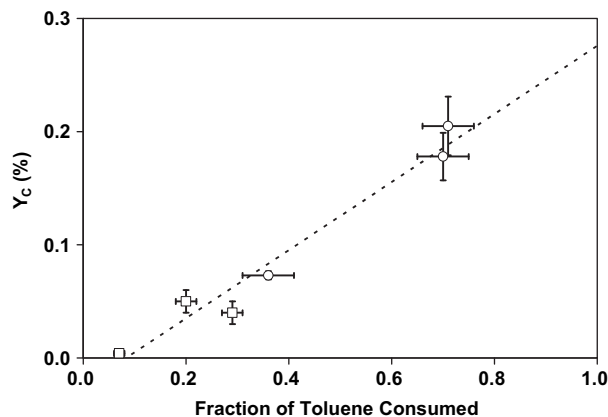**Fig. 5.** Plot for secondary POM carbon yield (Y_C) as function of fraction of toluene consumed observed in smog chamber experiments (circle) and flow reactor experiments (square). Circles are for this study and squares are adopted from Irei et al. (2006). The line shown is the linear regression from the Y_C points plotted ($r^2 = 0.963$).

a flow reactor (Irei et al., 2006), however, it should be noted that the one data point from the literature (i.e., the Y_C point at 15% of fraction of toluene consumed) was excluded in this plot due to the fact that true concentration measurements were not made for this data point only (Irei et al., 2006). The figure indicates that under our experimental conditions all the Y_C points are highly correlated with the fraction of toluene consumed ($r^2 = 0.963$), regardless of different initial toluene concentrations (~ 40 times lower), different toluene to NO_x ratios (~ 60 times higher), and introduction of seed particles. The linear regression obtained from this correlation is:

$$Y_C = (30.1 \pm 2.9)\frac{\Delta[C_{C7H8}]}{{}^{0}[C_{C7H8}]} - (2.5 \pm 1.3) \qquad (3)$$

As Y_C is $[C_{POM}]/\Delta[C_{C7H8}]$, Equation (3) can also be expressed as follows:

$$[C_{POM}] = (30.1 \pm 2.9)\frac{\Delta[C_{C7H8}]^2}{{}^{0}[C_{C7H8}]} - (2.5 \pm 1.3)\Delta[C_{C7H8}] \qquad (4)$$

As seen in Equation (4), $[C_{POM}]$ has a polynomial function of $\Delta[C_{C7H8}]$. Such a profile has been observed in the early stage of POM mass formation by others (Izumi and Fukuyama, 1990; Hurley et al., 2001; Sato et al., 2004). It should be pointed out that in their studies the plot for the POM mass and the carbon yields leveled off after some extent of toluene consumption. Although such a curving point was not observed here, it is possible that the linear trend shown in Fig. 4 may eventually level off when the studies are extended to further toluene consumption.

Comparison between the C_{POM} and the POM mass loaded on the filter ($^{loaded}M_{POM}$) gives an idea for carbon content of the POM. Similarly to Equation (1), the $^{loaded}M_{POM}$ for each filter sample was estimated using the sampling flow rate and the data for the POM mass concentration measured during the filter sampling. The comparison between the measured C_{POM} and the estimated $^{loaded}M_{POM}$ reveals that, on average, the estimated carbon content is $(27 \pm 4)\%$. The carbon content is lower than expected for the secondary POM produced by the photooxidation of toluene: i.e. the 49% carbon content found by Izumi and Fukuyama (1990) and the content of $> \sim 40\%$ for the specific products observed (Gery et al., 1985; Forstner et al., 1997; Jang and Kamens, 2001; Kleindienst et al., 2004; Sato et al., 2007). There are two possible explanations for the low carbon content: sampling artifact and substantial contribution of heteroatoms.

The loss of semi-volatile organic component during the filter sampling is an artifact causing low carbon contents in the method described above. Unfortunately, it is very difficult to evaluate sampling loss quantitatively at filter face. However, in our case, there are some implications that the impact of the sampling loss was likely small due to the following reasons: (1) the observed carbon contents for the three experiments were consistent, (2) no shift in the size distribution of the POM was observed during the filter sampling from the smog chamber where dry clean air was displaced (Irei, 2008), and (3) the very small loss of the POM carbon was observed during the sampling loss tests (Irei, 2008). These evidences imply that the POM was made of low volatile compounds, suggesting that the impact of the evaporation loss is small. Another possible explanation for the low carbon content is that the POM contained substantial amount of heteroatoms. Possible compound(s) that satisfy our observations are PAN type organic products or inorganic products, such as nitric and nitrous acids. Although the latter case is less likely due to their high vapor pressure, its possibility cannot be excluded since we did not actually analyze the acids. For confirmation of heteroatom contribution, further composition studies are needed.

3.3. Estimation of POM yield using stable carbon isotope ratio

The yield profile constructed (i.e. Equation (3) or Equation (4)) can be combined with the following Rayleigh type isotope fractionation in a closed system:

$$\frac{\Delta[C_{C7H8}]}{{}^0[C_{C7H8}]} = 1 - \left(\frac{\delta^{13}C_{C7H8} + 1000}{{}^0\delta^{13}C_{C7H8} + 1000} \right)^{\frac{{}^{OH}\varepsilon_{C7H8} + 1000}{{}^{OH}\varepsilon_{C7H8}}} \quad (5)$$

Since ${}^{OH}\varepsilon_{C7H8}$ and ${}^0\delta^{13}C_{C7H8}$ are known parameters here, Equation (5) allows estimating $\Delta[C_{C7H8}]/{}^0[C_{C7H8}]$ by measuring $\delta^{13}C_{C7H8}$ only, which in turn gives an estimation of Y_C by applying the $\Delta[C_{C7H8}]/{}^0[C_{C7H8}]$ to Equation (3).

The Y_C can also be expressed without the ${}^{OH}\varepsilon_{C7H8}$. In a closed system, the following mass balance must be conserved:

$$ {}^0[C_{C7H8}] = \Delta[C_{C7H8}] + [C_{C7H8}] \quad (6)$$

$$ {}^0\delta^{13}C_{C7H8} = \frac{\Delta[C_{C7H8}]}{{}^0[C_{C7H8}]}\delta^{13}C_{C7H8} + \left(1 - \frac{\Delta[C_{C7H8}]}{{}^0[C_{C7H8}]}\right)\delta^{13}C_{AllProd} \quad (7)$$

Using the two equations, Y_C can be expressed as follows (Irei et al., 2004; Irei, 2008):

$$ Y_C = \frac{{}^0\delta^{13}C_{C7H8}(‰) - \delta^{13}C_{AllProd}(‰)}{\delta^{13}C_{C7H8}(‰) - {}^0\delta^{13}C_{C7H8}(‰)} \cdot \frac{[C_{POM}]}{[C_{C7H8}]} \quad (8)$$

In the right side of this equation, the first division expressed with the isotope ratios physically means a variable that converts the $[C_{C7H8}]$ shown in the second division to the $\Delta[C_{C7H8}]$. Our results demonstrate that the $\delta^{13}C_{AllProd}$ is replaceable with the $\delta^{13}C_{POM}$, therefore, without knowing the KIE the Y_C can be determined by measuring the concentrations and the isotope ratios for toluene and the secondary POM after the reaction.

4. Summary

The results here demonstrate that under our experimental conditions the carbon KIE at the initial reaction step determines the stable carbon isotope ratio of the secondary POM formed by the toluene + OH reaction. The observed isotope ratios were distinctive from that of parent hydrocarbon, toluene. The results from the POM mass and carbon mass measurements ranged from 38% to 57% and from 7% to 21%, respectively. The difference suggests that the POM consists of heteroatom substantially. The yield plot here indicates the POM carbon yields obtained from different initial experimental conditions could be reasonably merged into a single profile. The shape of yield profile indicates that the POM consists of a second generation product, the production of which is likely limited by reactions with OH radicals. Using the experimental results here the yield of secondary POM can quantitatively be estimated by two independent approaches: one combining the observed yield profile with measurements for isotope ratios of toluene and another constructed according to mass balance, which requires measurements for the concentration and isotope ratios of toluene and secondary POM. When our experimental conditions are applicable to the atmosphere, those approaches will be applicable to ambient measurements.

Acknowledgement

References

Aggarwal, S., Kawamura, K., 2009. Carbonaceous and inorganic composition in long-range transported aerosols over northern Japan: implication for aging of water-soluble organic fraction. Atmospheric Environment 43, 2532–2540.

Anderson, R.S., Iannone, R., Thompson, A.E., Rudolph, J., Huang, L., 2004. Carbon kinetic isotope effects in the gas-phase reactions of aromatic hydrocarbons with the OH radical at 296 ± 4 K. Geophysical Research Letters 31. doi:10.1029/2004GL020089.

Anderson, R., 2005. Carbon kinetic isotope effects in the gas-phase reactions of nonmethane hydrocarbons with hydroxyl radicals and chlorine atom. Ph.D. Dissertation, York University, Toronto, Canada, pp. 1–257.

Anderson, T.L., Charlson, R.J., Schwartz, S.E., Knutti, R., Boucher, O., Rodhe, H., Heintzenberg, J., 2003. Atmospheric science: climate forcing by aerosols-a hazy picture. Science 300, 1103–1104.

Barbu, A.M., February, 2003. Smog chamber studies of aromatic hydrocarbon photooxidation by HO radicals. M.Sc. Thesis, York University, Toronto, Canada, 1–104.

Bienenstock, Y., May, 2001. Chamber studies of particulate production from HO reactions with toluene. M.Sc. Thesis, York University, Toronto, Canada, 1–153.

Dockery, D.W., Pope 3rd, C.A., Xu, X., Spengler, J.D., Ware, J.H., Fay, M.E., Ferris Jr., B.G., Speizer, F.E., 1993. An association between air pollution and mortality in six U.S. cities. New England Journal of Medicine 329, 1753–1759.

Edney, E.O., Driscoll, D.J., Speer, R.E., Weathers, W.S., Kleindienst, T.E., Li, W., Smith, D.F., 2000. Impact of aerosol liquid water on secondary organic aerosol yields of irradiated toluene/propylene/NOx/(NH4)2SO4/air mixtures. Atmospheric Environment 34, 3907–3919.

Fang, J., Kawamura, K., Ishimura, Y., Matsumoto, K., 2002. Carbon isotopic composition of fatty acids in the marine aerosols from the western north pacific: implication for the source and atmospheric transport. Environmental Science and Technology 36, 2598–2604.

Fisseha, R., Saurer, M., Jaggi, M., Siegwolf, R.T.W., Dommen, J., Szidat, S., Samburova, V., Baltensperger, U., 2009a. Determination of primary and secondary sources of organic acids and carbonaceous aerosols using stable carbon isotopes. Atmospheric Environment 43, 431–437.

Fisseha, R., Spahn, H., Wegener, R., Hohaus, T., Brasse, G., Wissel, H., Tillmann, R., Wahner, A., Koppmann, R., Kiendler-Scharr, A., 2009b. Stable carbon isotope composition of secondary organic aerosol from ß-pinene oxidation. Journal of Geophysical Research Atmosphere 114. doi:10.1029/2008JD011326.

Forstner, H.J.L., Flagan, R.C., Seinfeld, J.H., 1997. Secondary organic aerosol from photooxidation of aromatic hydrocarbons: molecular composition. Environmental Science and Technology 31, 1345–1358.

Gery, M.W., Fox, D.L., Jeffries, H.E., Stockburger, L., Weathers, W.S., 1985. A continuous stirred tank reactor investigation of the gas-phase reaction of hydroxyl radicals and toluene. International Journal of Chemical Kinetics 17, 931–955.

Grosjean, D., 1984. Atmospheric reactions of ortho cresol: Gas phase and aerosol products. Atmospheric Environment – Part A General Topics 18, 1641–1652.

Huang, L., Norman, A.L., Allison, C.E., Francey, R.J., Ernst, D., Chivulescu, A., Higuchi, K., 2001. Traceability – maintenance for high precision stable isotope measurement (δ¹³C & δ¹⁸O) of Air-CO2 by Lab-Carbonate-Standards at MSC: Application to the Inter-Comparison Program (alert, Canada) with CSIRO. In: the 11th WMO/IAEA Meeting of Experts on CO2 Concentration and Related Tracer Measurement Techniques, pp. 9–16.

Huang, L., Brook, J.R., Zhang, W., Li, S.M., Graham, L., Ernst, D., Chivulescu, A., Lu, G., 2006. Stable isotope measurements of carbon fractions (EC/OC) in airborne particulate: a new dimension for source characterization and apportionment. Atmospheric Environment 40, 2690–2705.

Hurley, M.D., Sokolov, O., Wallington, T.J., Takekawa, H., Karasawa, M., Klotz, B., Barnes, I., Becker, K.H., 2001. Organic aerosol formation during the atmospheric degradation of toluene. Environmental Science and Technology 35, 1358–1366.

Iannone, R., 2008. Laboratory and ambient studies of carbon isotope fractionation for atmospheric reactions of isoprene and other volatile organic compounds. Ph.D. Dissertation, York University, Toronto, Canada, 1–203.

Intergovernmental Panel on Climate Change, 2001. Climate Change 2001: The Scientific Basis.

Irei, S., Huang, L., Collin, F., Zhang, W., Hastie, D., Rudolph, J., 2004. Flow reactor studies for stable carbon isotopic composition of secondary particulate organic matter generated by toluene/OH radical-initiated reactions. Abstract of The 16th International Conference on Nucleation and Atmospheric Aerosols, Kyoto, Japan.

Irei, S., Huang, L., Collin, F., Zhang, W., Hastie, D., Rudolph, J., 2006. Flow reactor studies of the stable carbon isotope composition of secondary particulate matter generated by OH-radical-induced reactions of toluene. Atmospheric Environment 40, 5858–5867.

Irei, S. 2008. Laboratory studies of stable carbon isotope ratio of secondary particulate organic matter. Ph.D. Dissertation, York University, Toronto, Canada, 1–132.

Izumi, K., Fukuyama, T., 1990. Photochemical aerosol formation from aromatic hydrocarbons in the presence of nitrogen oxides (NO_x). Atmospheric Environment, Part A: General Topics 24A, 1433–1441.

Jang, M., Kamens, R.M., 2001. Characterization of secondary aerosol from the photooxidation of toluene in the presence of NO_x and 1-propene. Environmental Science and Technology 35, 3626–3639.

Kleindienst, T.E., Conver, T.S., McIver, C.D., Edney, E.O., 2004. Determination of secondary organic aerosol products from the photooxidation of toluene and their implications in ambient PM2.5. Journal of Atmospheric Chemistry 47, 79–100.

Lee, P.K.H., Brook, J.R., Dabek-Zlotorzynska, E., Mabury, S.A., 2003. Identification of the major sources contributing to POM2.5 observed in Toronto. Environmental Science and Technology 37, 4831–4840.

Na, K., Sawant, A.A., Song, C., Cocker, D.R., 2004. Primary and secondary carbonaceous species in the atmosphere of western Riverside County, California. Atmospheric Environment 38, 1345–1355.

Nara, H., Toyoda, S., Yoshida, N., 2007. Measurements of stable carbon isotopic composition of ethane and propane over the western north pacific and eastern Indian ocean: a useful indicator of atmospheric transport process. Journal of Atmospheric Chemistry 56, 293–314.

Noyes, W.A., 1943. n-butyl nitrite. Organic Syntheses 2, 108–109.

Odum, J.R., Hoffmann, T., Bowman, F., Collins, D., Flagan, R.C., Seinfeld, J.H., 1996. Gas/particle partitioning and secondary organic aerosol yields. Environmental Science and Technology 30, 2580–2585.

Ramanathan, V., Crutzen, P.J., Kiehl, J.T., Rosenfeld, D., 2001. Atmosphere aerosols, climate, and the hydrological cycle. Science 294, 2119–2124.

Rudolph, J., Czuba, E., Huang, L., 2000. The stable carbon isotope fractionation for reactions of selected hydrocarbons with OH-radicals and its relevance for atmospheric chemistry. Journal of Geophysical Research, Atmospheres 105, 29329–29346.

Rudolph, J., Czuba, E., Norman, A.L., Huang, L., Ernst, D., 2002. Stable carbon isotope composition of nonmethane hydrocarbons in emissions from transportation related sources and atmospheric observations in an urban atmosphere. Atmospheric Environment 36, 1173–1181.

Saito, T., Tsunogai, U., Kawamura, K., Nakatsuka, T., Yoshida, N., 2002. Stable carbon isotopic compositions of light hydrocarbons over the western north pacific and implication for their photochemical ages. Journal of Geophysical Research, Atmosphere 107, (D4), 4040. doi:10.1029/2000JD000127.

Sakugawa, H., Kaplan, I.R., 1995. Stable carbon isotope measurements of atmospheric organic acids in los Angeles, California. Geophysical Research Letters 22, 1509–1512.

Sato, K., Klotz, B., Hatakeyama, S., Imamura, T., Washizu, Y., Matsumi, Y., Washida, N., 2004. Secondary organic aerosol formation during the photooxidation of toluene: dependence on initial hydrocarbon concentration. Bulletin of the Chemical Society of Japan 77, 667–671.

Sato, K., Hatakeyama, S., Imamura, T., 2007. Secondary organic aerosol formation during the photooxidation of toluene: NO_x dependence of chemical composition. Journal of Physical Chemistry A 111, 9796–9808.

Stroud, C.A., Makar, P.A., Michelangeli, D.V., Mozurkewich, M., Hastie, D.R., Barbu, A., Humble, J., 2004. Simulating organic aerosol formation during the photooxidation of Toluene/NO_x mixtures: comparing the equilibrium and kinetic assumption. Environmental Science Technology 38, 1471–1479.

Thompson, A., Rudolph, J., Rohrer, F., Stein, O., 2003. Concentration and stable carbon isotopic composition of ethane and benzene using a global three-dimensional isotope inclusive chemical tracer model. Journal of Geophysical Research, [Atmosphere] 108, 4373. doi:10.1029/2002/JD002883.

Thurston, G.D., Ito, K., Hayes, C.G., Bates, D.V., Lippomann, M., 1994. Respiratory hospital admissions and summertime haze air pollution in Toronto, Ontario: consideration of the role of acid aerosols. Environmental Research 65, 271–290.